A NEW GEOMETRY HIGH PERFORMANCE LOW POWER MCFC

Franco Cotana (1), Federico Rossi (2), Andrea Nicolini (3)

(1) Università degli Studi di Perugia, Dipartimento di Ingegneria Industriale, Via G. Duranti 67, 06125 Perugia, Italy, Ph. +39 075 5853717, Fax +39 075 5853697, E-mail:cotana@unipg.it

(2) Università degli Studi di Perugia, Dipartimento di Ingegneria Industriale, Via G. Duranti 67, 06125 Perugia, Italy, Ph. +39 075 5853846, Fax +39 075 5848470, E-mail: frossi@unipg.it

(3) Corresponding Author, Università degli Studi di Perugia, Dipartimento di Ingegneria Industriale, Via G. Duranti 67, 06125 Perugia, Italy, Ph. +39 075 5853845, Fax +39 075 5848470, E-mail: nicolini.unipg@ciriaf.it

ABSTRACT

Molten Carbonate Fuel Cells (MCFC) working temperatures are 600-700°C; thus, MCFC are characterized by high energy conversion efficiency. However, only large size MCFC (from kW hundreds to MW tens power range) are actually realized, both for economic and technical reasons. A new geometry small size MCFC is here proposed. Cell thermofluidodynamical performances have been analyzed by means of a numerical code. Simulations results verified the suitability of the proposed cell design solutions. A stack constituted by three elementary units has been realized in order to experimentally evaluate the proposed cell performances.

INTRODUCTION

Energy saving and enviromental problems have recently focused the operators to develop cogenerative energy systems able to simultaneously generate electric and thermal energies. In Europe, energy market liberalization (according to European Directive 96/92/EC [1]) has encouraged the development of low power cogenerative systems for small and medium users energetic requirements. These systems are characterized by high global efficiency and low installation, management and maintenance costs. Fuel cells are an electrochemical system able to generate electric energy by fuel chemical energy; no intermediate thermal cycles occur (differently from traditional thermal machines). Molten Carbonate Fuel Cells (MCFC) are characterized by high working temperatures (600-700°C); thus, high benefits may be obtained in terms of efficiency and chemical reactions kinetics. Economic and technical reasons have actually allowed to develop only high power MCFC, from kW hundreds to MW tens power range [2]. A low power original MCFC is here proposed [3]. A new geometry characterizes the proposed cell elements (anode, cathode and matrix). Thus, benefits may be obtained in terms of: realization times and costs; thermal dispersion minimization; global efficiency; minimization of gases retaining among the cell plates; compression strain sharing uniformity on the contact surface. The proposed cell design solutions have been verified by numerical simulations which have allowed to individuate inner-cell temperature, pressure and velocity distributions. A measurement campaign is actually going on in order to verify the thermofluidodynamic performances of a stack constituted by three elementary units.

3. THE PROPOSED MCFC

A low power MCFC is here proposed. The cell is fed by methane; it is characterized by a new geometry and innovative thermofluidodynamic working peculiarities. The proposed cell is constituted by a stack, a catalytic burner and a start-up burner (see Fig. 1). Stack is made up by elementary electrochemical cells (each constituted by anode, cathode and matrix) characterized by a circular base cylindrical shape. Each elementary unit is constituted by two different cylindrical sections. Anodic section is placed in the elementary unit bottom portion; fuel gas mixed with steam flows in it (ref. 15, Fig. 1). Cathodic section is placed in the elementary unit upper portion; an air-carbonic anhydride (the comburent) mixture flows in it (ref. 17, Fig. 1). Anodic section is made up by two overlying sections obtained by interposing a centre-holed separating plate (ref. 7, Fig. 1). A nickel based catalyser is deposited on ceramic pellets in the anode bottom section (ref. 5, Fig. 1); an endothermic reforming reaction occurs in this section which allows to obtain hydrogen and carbon monoxide from methane. In the anode upper section, a H_2 - CO mixture contacts the nickel-chrome porous anode (ref. 1, Fig. 1). The proposed configuration allows to make thermal energy produced by cell electrochemical reactions available for reforming reaction. In the cathodic sections, comburent gases contact the nickel oxide porous cathode (ref. 2, Fig. 1). The matrix is constituted by a lithium aluminate porous element which is soaked in lithium and potassium carbonates (ref. 3, Fig. 1). In the anodic upper section, hydrogen combines with the electrolyte carbonate ion; H_2O, CO_2 and electrons are the reaction products. Hydrogen is obtained both by methane-steam reaction (reforming, which occurs in the anode bottom section) and by CO-steam reaction (shift reaction, which occurs in the anode upper section). In the cathodic sections, oxygen combines with CO_2 regenerating the carbonate ion. Global electrochemical reaction is exothermic. Thus, the elementary cell chemical reactions are:

$$CH_4 + H_2O \rightarrow CO + 3H_2 \qquad \text{(methane reforming reaction)} \tag{1}$$

$$CO + H_2O \rightarrow CO_2 + H_2 \qquad \text{(shift reaction; it occurs in the anodic section)} \tag{2}$$

$$H_2 + CO_3^{--} \rightarrow H_2O + CO_2 + 2e^- \qquad \text{(anodic reaction)} \tag{3}$$

$CO_2 + 1/2O_2 + 2e^- \rightarrow CO_3^{--}$ (cathodic reaction) (4)

Gases inlets (ref. 19 and 22, Fig. 1) and outlets (ref. 20 and 21, Fig. 1) are placed on the stack lateral surface. A double path is designed for each elementary unit both for anodic and cathodic flows: it converges from the external surface to the cell centre in the entry phase; it is opposite during the exit phase. It is obtained by inserting a separator plate for each semi-cell. Flow inversion occurs by a vertical hole placed in the separator plate centre. Electrochemical reactions between gases and electrodes occur during the exit paths. An uniform gases distribution is obtained by realizing some holes placed symmetrically on the cell external surface. Gases are distributed on a 360° angle by realizing a circular corona shape path on the separator plates zone external to the electrodes (ref. 6, Fig. 1). These paths are the cell internal distribution collectors. Concentric circular canals are obtained in the separator plates zone internal to the electrodes one by realizing decreasing radius annular protrusions (ref. 4, Fig. 1). Each canal is connected to the adjacent one by means of radial crossings; each protrusion is characterized by the same crossing number distanced each other by the same α angle. Consecutive protrusions openings are staggered by a $\beta = \alpha/2$ angle in order to avoid preferential paths and no-flow zones. A particular collector system is integrated with the steel coat which externally covers the proposed cell. Steel diaphragms divided longitudinally the space between the steel cylindrical coat and the cell. Diaphragms are united to the steel coat; ceramic linings are placed on the cell side in order to obtain high gases retaining and electric insulation. Exhaust sections are double than feeding ones both for anodic and cathodic flows; damages due to gases escapes are minimized by realizing each inlet collector placed between two same outlet collectors (ref. 19, 20, 21 and 22, Fig. 1). Thus, an eventual gas escape follows from the feeding collector to the exhaust one, because gas pressure in the inlet collector is higher than in the outlet one. A circular base cylindrical shape catalytic burner is placed over the electrochemical stack. Catalytic burner allows to: recuperate carbonic anhydride produced into the anodic sections (ref. 16, Fig. 1) in order to feed the cathodic sections; eliminate fuel residues in the exhaust anodic gases (methane, hydrogen, CO) by catalytic combustion. Catalyser is nickel deposed on a ceramic support (ref. 8, Fig. 1). Cathodic reaction is fed by O_2 obtained by air (ref. 18, Fig. 1) which enters in the catalytic burner central zone; the following reactions occur:

$CH_4 + 2O_2 \rightarrow CO_2 + 2H_2O$ (methane combustion) (5)

$CO + 1/2O_2 \rightarrow CO_2$ (CO combustion) (6)

$H_2 + 1/2O_2 \rightarrow H_2O$ (hydrogen combustion) (7)

A modulable power ceramic start-up burner (ref. 9 and 10, Fig. 1) is placed under the stack. Start-up burner allows to: generate the hot gases (ref. 11, Fig. 1) to be led to the cathodic section together with the anodic exhaust (ref. 16, Fig. 1); fuel heating (ref. 14, Fig. 1) and water vaporization (ref. 12, Fig. 1) in order to realize reforming reaction in the anodic section. Start-up burner maximum working conditions occur only in the start-up phase in order to produce the stack nominal temperature. It contributes only to the gases pre-heating when the stack nominal conditions have been achieved. The proposed cell main peculiarity is relative to the geometry which characterizes the elementary units elements (anode, cathode and matrix). High benefits may be obtained by this configuration. The small area cylindrical elements may be easily obtained by injection printing; this is a moulding technique which is conveniently used for large scale productions, with high times and costs advantages. Cylindrical configuration contributes also to reduce thermal dispersions thank to this geometry intrinsic properties and its insulation easiness. Besides, gases retaining problem is reduced and the compression strain is uniformly shared on the contact surface.

THEORETICAL INDIVIDUATION OF THE PROPOSED CELL PERFORMANCES

Gases flow rates and compositions relative to each elementary cell section (internal reformer, anode and cathode) have been theoretically evaluated. Equations (1-7) have been used by taking into account chemical reactions evolution and cell configuration. The following hypotheses have been assumed: constant current density on all electrodes surface; fuel is constituted by pure methane; shift reaction occurs completely in the anodic section because is here furthered by the hydrogen consumption and the steam generation; no conversions occur when methane residues from the reformer contact the anode (very low CH_4 solubility relative to molten carbonates); anodic exhaust fuel residues are completely converted by catalytic combustion; air molar composition at the catalytic burner inlet is O_2 (21%), N_2 (79%); no reactions occur relatively to N_2; carbonic anhydride flow rate at the cathodic inlet has been evaluated by assuming a complete anodic exhaust recycle. Cell design parameters values have been determined by means of thermodynamic evaluations on the chemical reactions and MCFC experimental results [4]. Nominal current density design value is 150 mA/cm^2. Reforming is fed by the following methane-steam mixture: $CH_4 = 33\%$; $H_2O = 67\%$. This composition value has been obtained by considering the steam-methane molar ratio able to feed reforming and shift reaction. Besides, this configuration avoids the carbon deposition on the catalyser for 1 atm pressure and 650 °C temperature operative conditions [5]. Equilibrium constant k_{ref} relative to methane steam reforming may be expressed in terms of X (converted methane moles) [6]:

$$k_{ref} = \frac{X \cdot (3X)^2 P^2}{(F_{CH_4} - X) \cdot (F_{CH_4} \cdot s/c - X) \cdot [F_{CH_4}(1 + s/c) + 2X]^2} \tag{8}$$

By considering $k_{ref}=2.85\ atm^2$ [6], P=1atm, s/c=2 (steam-methane ratio), $F_{CH4}=1$ (methane molar rate at the reformer inlet), Eq. (8) gives X=0.83; this value corresponds to methane utilisation degree (U_{CH4}), if equilibrium conditions are assumed to be obtained in the reformer. Similarly, by considering anodic electrochemical reaction (see Eq.(3)), shift reaction balance constant k_{sr} may be expressed in terms of Y (CO moles used by shift reaction) [6]:

$$k_{sr} = \frac{[Y + (3X + Y) \cdot U_{H_2}] \cdot [(3X + Y) \cdot (F_{CH_4} - U_{H_2})]}{[X - Y] \cdot [2 - X - Y + (3X + Y) \cdot U_{H_2}]} \tag{9}$$

By considering k_{sr}=2.08 atm^2 [6] and hydrogen utilisation degree (H_2 moles which take part to the anodic electrochemical reaction compared to the ones produced by reforming and shift reaction per time unit) U_{H2} = 0.8 (optimal value determined by 150 mA/cm^2 current density value), Y is 0.54. Y/X=0.66 represents CO fraction which is transformed by shift reaction when its kinetic allows to obtain equilibrium conditions at the anodic outlet; this condition is difficultly obtainable because gases composition at the anodic upper section varies very quickly due to the contemporaneous electrochemical reaction. Thus, U_{CO} (carbon monoxide utilisation degree) has been assumed lower (0.55) than the optimum one. U_{O2} (oxygen utilisation degree) determines air flow rate at the cathodic inlet; its value depends on the cathodic reaction stechiometry and the cell refrigeration requirements. In fact, inlet air flow is usually used as refrigerant. A value greater than the MCFC designed until now has been assumed (U_{O2} = 0.42) [5]. Gases flow rates, species consumption and generation have been evaluated relatively to a 30 cm diameter electrodes single cell (see Tab. 1 and 2).

Table 1: *Gases Flow rates and composition (30 cm diameter electrodes single cell)*

Cell Zone	*Molar Flow Rate mol/sec*	*Molar Composition mol/mol*	*Mass Flow Rate kg/sec*	*Mass Composition kg/kg*
Reformer inlet	6.993e-4	CH_4: 0.333 H_2O: 0.667	1.212e-5	CH_4: 0.308 H_2O: 0.692
Reformer outlet	1.086e-3	CH_4: 0.036 H_2O: 0.251 H_2: 0.534 CO: 0.178	1.212e-5	CH_4: 0.052 H_2O: 0.404 H_2: 0.096 CO: 0.447
Anodic outlet	1.636e-3	CH_4: 0.024 H_2O: 0.438 H_2: 0.084 CO: 0.053 CO_2: 0.401	4.509e-5	CH_4: 0.014 H_2O: 0.286 H_2: 0.006 CO: 0.054 CO_2: 0.640
Cathodic inlet	4.834e-3	O_2: 0.135 CO_2: 0.162 H_2O: 0.045 N_2: 0.658	1.483e-4	O_2: 0.141 CO_2: 0.232 H_2O: 0.026 N_2: 0.601
Cathodic outlet	4.010e-3	O_2: 0.095 CO_2: 0.058 H_2O: 0.054 N_2: 0.793	1.154e-4	O_2: 0.105 CO_2: 0.089 H_2O: 0.034 N_2: 0.772

The first principle of thermodynamics has been applied in order to evaluate heat produced or absorbed by the cell chemical reactions:

$$\Delta E = Q + W_{pv} + W_{el} \tag{10}$$

ΔE is the difference between products and reagents internal energies; W_{el}=0 relatively to reforming and shift reaction, because no electric work is produced. Molar reaction heat q has been calculated by the following relation

$$q = \sum_{1}^{Np} n_p h_p - \sum_{1}^{Nr} n_r h_r \tag{11}$$

The following results have been obtained:

$$
\begin{aligned}
q_{ref} &= [h(CO)+3h(H_2)]-[h(CH_4)+h(H_2O)] = 224.8\ \mathrm{kJ/mol}\ (CH_4) \\
q_{sr} &= [h(CO_2)+h(H_2)]-[h(CO)+h(H_2O)] = -35.5\ \mathrm{kJ/mol}\ (CO)
\end{aligned}
\tag{12}
$$

q_{ref} and q_{sr} values show that methane steam reforming and shift reaction are respectively an endothermic and a slight exothermic process. Equation (11) may be rewritten relatively to the electrochemical process:

$$
\Delta h = \sum_{1}^{Np} n_p h_p - \sum_{1}^{Nr} n_r h_r = q_{el} + w_{el} \tag{13}
$$

Table 2: *Chemical species consumption and generation*

Cell Zone	*Reaction*	*Species*	*Consumption*		*Generation*	
			mol/sec	*kg/sec*	*mol/sec*	*kg/sec*
Reformer	Steam reforming	CH_4	1.935e-4	3.09e-6		
		H_2O	1.935e-4	3.48e-6		
		H_2			5.804e-4	1.16e-6
		CO			1.935e-4	5.42e-6
Anodic Section	Shift reaction	H_2O	1.064e-4	1.92e-6		
		H_2			1.064e-4	2.1e-7
		CO	1.064e-4			
		CO_2		2.98e-6	1.064e-4	4.68e-6
	Anodic Semi-reaction	H_2O			5.494e-4	9.89e-6
		H_2	5.494e-4	1.10e-6		
		CO_2			5.494e-4	2.418e-5
Cathodic Section	Cathodic Semi-reaction	CO_2	5.494e-4	2.418e-5		
		O_2	2.747e-4	8.79e-5		

Molar electric work w_{el} has been evaluated by electric charge and cell potential V [5]:

$$
w_{el} = -nFV \tag{14}
$$

Cell potential may be evaluated by considering reversible potential ε_{rev}; it represents the maximum potential difference between cell electrodes due to a reversible process. ε_{rev} has been evaluated by considering Gibbs energy Δg for an isotherm transformation [6]:

$$
\Delta g = w_{el} = -nF\varepsilon_{rev} \tag{15}
$$

Cell potential difference may be obtained by ε_{rev} and the current density j [6]:

$$
V = \varepsilon_{rev} - j\cdot(R_{ohm} + Z_a + Z_c) \tag{16}
$$

Z_a and Z_c are anodic and cathodic impedances, have been evaluated by known relations [6]. ε_{rev}, Z_a and Z_c depend on gases partial pressures which vary on the distributor plates due to the chemical reactions evolution. Thus, V is not uniformly distributed on electrodes surface; electric work has been evaluated by assuming a constant V value which is a weighted average value between potentials relative to five circular coronas in which the cell may be divided. V is 0.756V; the correspondent electric power per cell surface unit is 1130 W/m^2. A 3kW nominal electric power is obtained by stacking 38 elementary cells. By substituting V in Eq. (14):

q_{el} = -101.71 kJ/mole(H_2) (17)

Theoretical DC electric efficiency η_{el} is defined as the ratio between electric power generated by the cell and fuel energy introduced in the reforming section per time unit:

$$\eta_{el} = \frac{V \cdot j \cdot S}{F_{CH_4} \cdot I.C.P._{CH_4}} \qquad (18)$$

Global heat absorbed or generated by the elementary cell have been evaluated by multiplying reaction heat values q_{ref}, q_{sr} e q_{el} respectively with methane, CO and hydrogen molar consumption values: heat absorbed by reforming reaction is 43.5 W/cell; heat generated by shift reaction is 3.8 W/cell; heat generated by electrochemical reaction is 55.9 W/cell. Thus, cell global heat generation is 16.2 W/cell.

THE PROPOSED CELL NUMERICAL VALIDATION

The proposed cell thermofluidodynamic performances have been evaluated by a volume finite numerical code [7]. A simplified numerical model has been realized due to high complex phenomena which characterizes the proposed cell: a single elementary cell has been analyzed; stationary conditions have been considered; gases flows on distribution plates have been considered laminar both for cathodic and anodic section; external, upper and bottom surfaces have been considered adiabatic. Energy, mass, chemical species generation and absorption have been simulated by introducing sources and bores in the model. A cell eighth model has been simulated due to cell symmetry. Model has been meshed in 2506861 tetrahedral elements. The following boundary conditions have been assumed: reformer semi-inlet mass flow is 1.515e-6 kg/s (global cell one eighth); reformer semi-inlet gases composition has been individuated by Tab. 1 mass fractions; fuel and oxidant inlet temperatures are respectively 873K and 823K; cathodic entire inlet mass flow is 1.236e-5 kg/s (1/12 with respect to global cell one, see Fig. 2); cathodic semi-inlet mass flow is 6.18e-6 kg/s (1/24 with respect to global cell one, see Fig. 2); gases composition assumed for both cathodic inlets are O_2=0.141; CO_2=0.232; H_2O=0.026 (see Tab. 1); anodic and cathodic exhaust pressure is 1 atm. As an example, Figure 2 shows simulated temperatures, pressures and velocities distributions relative to anodic upper section and cathodic bottom section. Gases temperatures distribution is radial and varies in a 30K range. Highest temperature (930 K) is in the cell central zone near the inlet hole; lowest temperature (about 900 K both for anodic and cathodic gases) is in the cell external zone near the exhaust outlets, due to the adjacent feeding gases inlets. Gases pressures behaviour is radial both for anodic and cathodic sections. Highest pressure value is in the cell central zone (both for anodic and cathodic sections). Cathodic pressure range is lower than the anodic one due to the lower gas flow rate. In fact, heat produced by electrochemical reactions is partially absorbed by the internal reformer; thus, oxidant flow for refrigeration is reduced. Velocities behaviour shows that cathodic and anodic gases flows as designed. Numerical simulations results have shown that the adopted solutions (a new geometry and the innovative gases distribution system) are appropriate. Moreover, simulations have verified that: temperature differences among the cell zones are low (it allows to avoid the degradation phenomena in the hottest zones and to increase cell life); thermal integration between reforming and electrochemical sections is efficacious; cell internal distribution system allows to keep low pressure difference between cathodic and anodic section (gases cross-over is avoided [5]).

AN EXPERIMENTAL PROTOTYPE

An experimental prototype has been realized. It is constituted by a 3 elementary cell stack. Figure 3 shows a stack element (cathodic bottom section view). An experimental measurement campaign is actually going on in order to verify the cell performances given by numerical simulations.

CONCLUSIONS

A low power innovative MCFC has been proposed. The cell is characterized by an original cylindrical shape; gases flow rates and compositions have been evaluated relatively to the different cell sections. The following performances have been evaluated: theoretical electric efficiency is 0.427; 3kW electric power may be obtained by stacking 38 elementary cells. Design solutions efficacy has been verified by means of numerical simulations (in terms of temperatures, pressures and velocities). A cell constituted by three elementary units has been realized. A thermofluidodynamic measurement campaign is now going on in order to experimentally confirm the simulation results. The proposed cell applications are relative both to civil and industrial users; it may replace traditional gas or double feeding (gas + diesel) boilers as heating plant and simultaneously produce electric energy for the same user. High temperature heat produced by the proposed cell may be used to fed an absorption machine; a circuit dimensions reduction and a thermodynamical cycles energetic efficiencies increasing may be obtained. Thus, an energetic and economic estimation of the proposed MCFC for electric and thermal domestic users requirements will be evaluated.

NOMENCLATURE

Symbol	*Units*	*Description*
F	C/mol	Faraday constant
h_p, h_r	J/mol	Molar enthalpy relative to the p-th product, r-th reagent
n_p, n_r	mol	p-th product moles, r-th reagent moles
n	adimensional	Number of electrons
P	atm	Pressure
$P_{i,a}$, $P_{i,c}$	atm	i-th gas partial pressure in the anodic section, in the cathodic section
$I.C.P._{CH4}$	J/mol	Methane inferior calorific power
R_{ohm}	$\Omega \cdot m^2$	Impedance due to ohmic polarization
S	m	Electrode surface
W_{pv}	J	Mechanic work

REFERENCES

[1] The European Parliament and the Council of the European Union, 1996, “Directive 96/92/EC of the European Parliament and of the Council of 19 December 1996 concerning common rules for the internal market in electricity”.

[2] Hishinuma Y., Kunikata M., 1997, “Molten carbonate fuel cell power generation systems”, Energy Conversion and Management 38, Issue 10-13, pp. 1237-1247.

[3] IPASS, 2003, “Dispositivo termoelettrochimico a carbonati fusi per la generazione contemporanea di elettricità e calore a geometria cilindrica”, Ministero dell’Industria, del Commercio e dell’Artigianato, Patent N. PG2003A0019, Italy.

[4] Koh J., Seo H., Yoo Y., Lim H., 2002, “Consideration of numerical simulation parameters and heat transfer models for a molten carbonate fuel cell stack”, Chemical Engineering Journal 87, Issue 3, pp. 367-379.

[5] Freni S., Aquino M., Passalacqua E., 1994, “Molten carbonate fuel cell with indirect internal reforming”, Journal of Power Sources 52, Issue 1, pp.41-47.

[6] Hou K., Hughes R., 2001, “The kinetics of methane steam reforming over a Ni/α-Al$_2$O catalyst”, Chemical Engineering Journal 82, Issue 1-3, pp. 311-328.

[7] Fluent Incorporated, 1998, “Fluent 5 User Guide”.

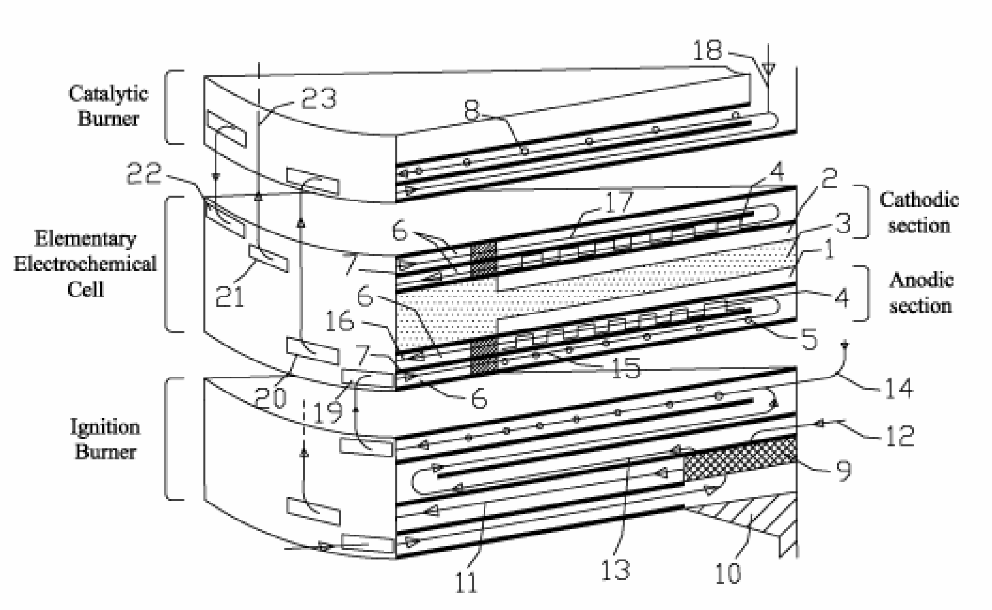

Figure 1: the proposed MCFC design scheme.

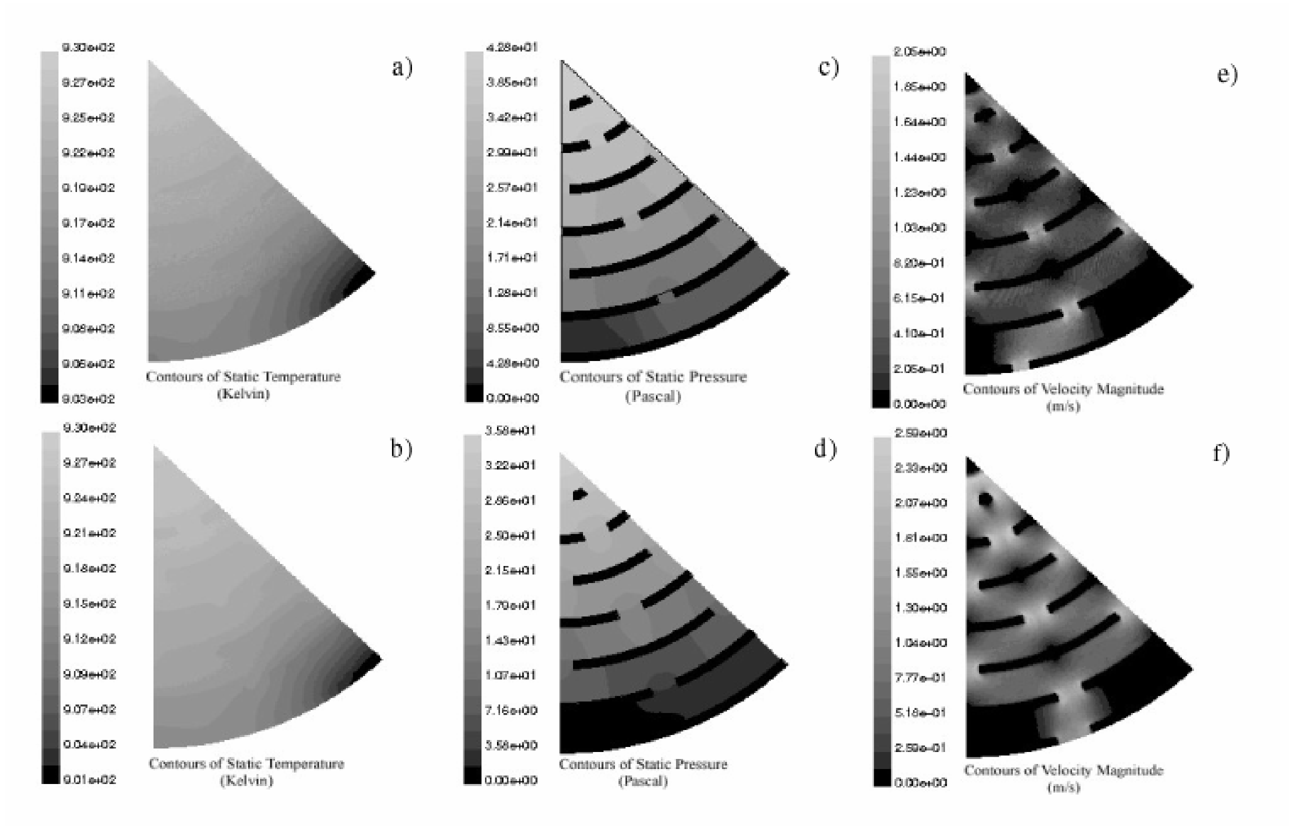

Figure 2: (a) anodic upper section temperature distribution; (b) cathodic bottom section temperature distribution; (c) anodic upper section pressure distribution; (d) cathodic bottom section pressure distribution; (e) anodic upper section velocity distribution; (f) cathodic bottom section velocity distribution.

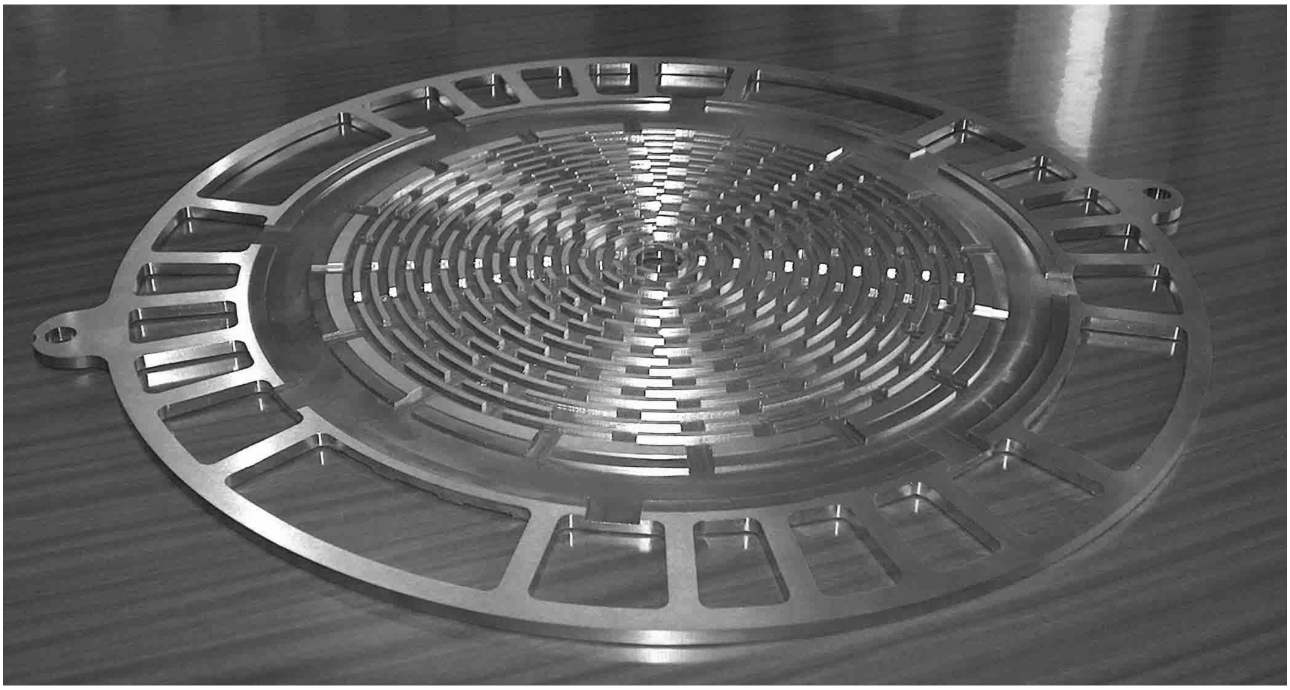

Figure 3: an element of the MCFC prototype (cathodic bottom section view)

FIGURE CAPTIONS

Figure 1: a) the proposed MCFC design scheme; b) distribution and exhaust collectors position.

Figure 2: (a) anodic upper section temperature distribution; (b) cathodic bottom section temperature distribution; (c) anodic upper section pressure distribution; (d) cathodic bottom section pressure distribution; (e) anodic upper section velocity distribution; (f) cathodic bottom section velocity distribution.

Figure 3: an element of the MCFC prototype (cathodic bottom section view)